Supporting information

SI 0: TEM & STEM acquisition parameters, in 2D and 3D

Electron tomography acquisitions were performed on a JEOL 2100F transmission electron microscope with a field emission gun and a post-column GATAN Tridiem energy filter. For the preparation of the TEM grids, the powders have been diluted in an ethanol solution and several droplets of the obtained solution have been deposited on the grids. The tilt series have been recorded in an automatic manner using the GATAN tomography software.

In the bright field mode, each tilt series has been recorded by covering an angular range between -70° an +70° with an increment of 2° following the Saxton scheme[1]. The TEM images are made of 2048×2048 pixels with a pixel size of 0.16 nm for the mesoporous silica-based sample and of 0.13 nm for the silica nanofiber. No visible beam damage was observed after the acquisition.

The HAADF-STEM tilt series was acquired using the ADF detector by tilting the specimen in the angular range of ± 70° using an increment of 2.5° in the equal mode, giving thus a total of 57 images in the series. The relatively large inner radius chosen for the ADF detector, 40 mrad, allowed us to consider that the intensity in the corresponding images scales with the mean atomic number. Finally, the gain of the ADF detector was chosen such that any saturation effect in the HAADF images during the series acquisition was prevented.

The alignment was applied employing IMOD software[2], the volumes computations were performed employing 15 iterations of algebraic reconstruction technique algorithm (ART)[3] implemented in TOMOJ/EFTETJ software[4] obtaining 512x512x512 pixels volumes. The 3D visualization, surface rendering and various parameters quantification were performed combining different tools implemented in the software ImageJ, 3D Slicer[5] and Chimera[6].

SI 1: Mesoporous hollow-shell mixed oxide nanoparticles

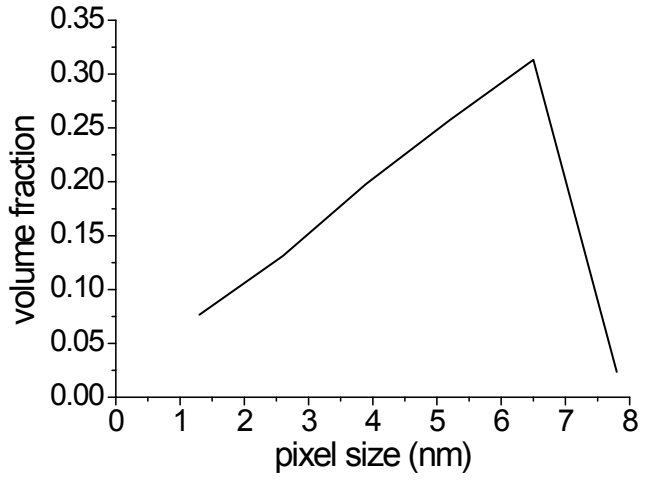

Figure S1: Pore size distribution.

SI 2: 3D mesoporous fibers

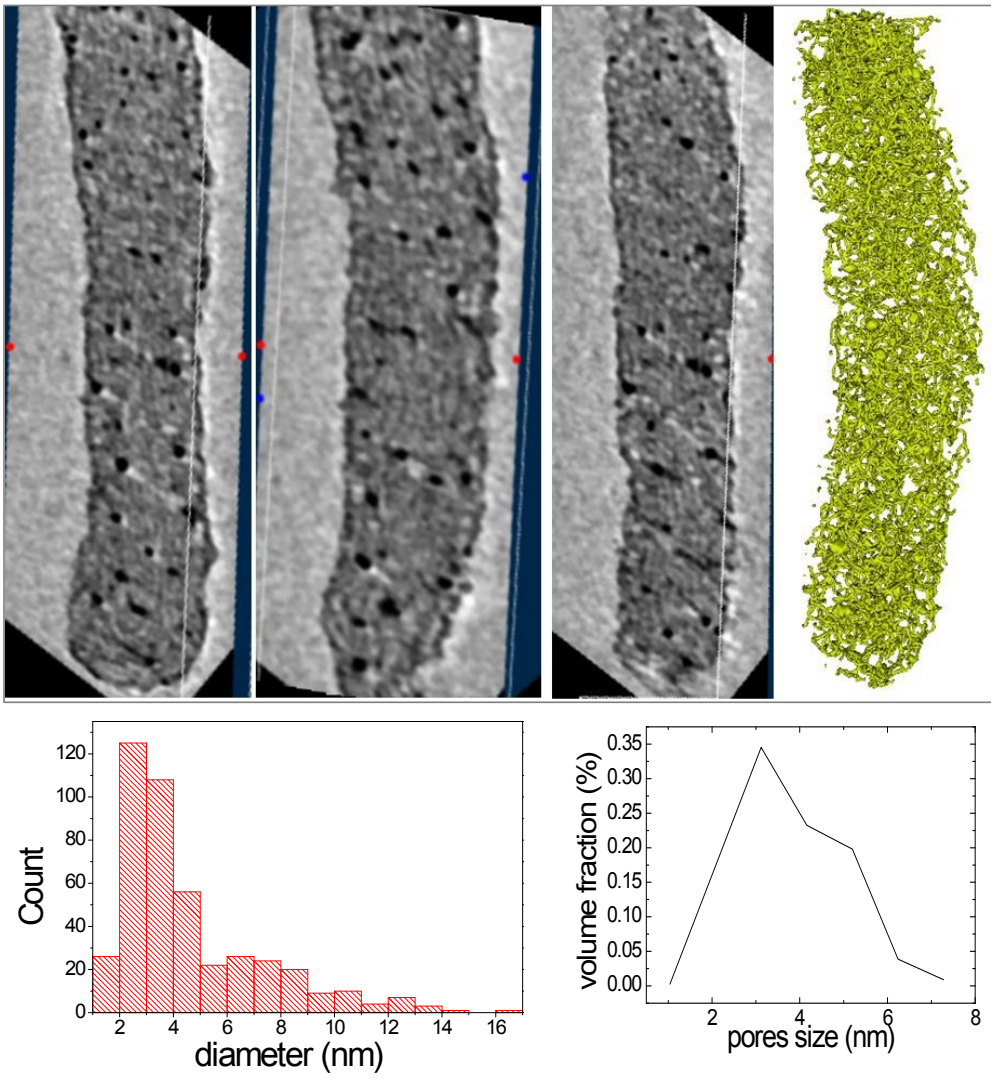

Figure S2: a) Typical longitudinal slices showing the helicoidal orientation of the pores and a 3D image of the lateral connections. b) Au particles size distribution. c) Pore size distribution.

SI 3: Multiple phosphorus species in Ni-P nanoparticles

SI 3.1. Choice of the experimental conditions and the P elemental 2D map calculation

The EFTEM tomographic tilt series were recorded by using the GATAN acquisition software on the JEOL 2100 F electron microscope by tilting the specimen over a relatively reduced angular range (±60). Four energy filtered images were recorded at each tilt angle: the Zero-Loss filtered image, a non-filtered image and the two filtered images for the phosphorus L2,3 ionization edge: the pre-edge image at 120 eV and a post-edge image at 152 eV. The slit width used for the acquisition of the ZL images was 10 eV, whereas the slit width used for acquisition of the phosphorus elemental projection was 20 eV.

Regarding the exposure time, since the phosphorus signal is relatively weak, the exposure time used to record the filtered images was long enough in order to achieve high signal to noise ratio (SNR) in the final elemental projection tilt series. For that we have used a time exposure of 10 s for each filtered image and 0.5s for each image belonging to the ZL tilt series. The non-filtered TEM tilt series was acquired for correcting the object drift during the whole acquisition process. The reduced angular range (±60) is limited by the configuration of the cryogenic sample holder. For the alignment of all the tilt series the procedure described in reference 1 was used in order to correct a possible drift of the object during the acquisition of the tilt series.

For the calculation of the P elemental map since we have only two filtered images, we used the method proposed by Leapman and al.[7] described here below.

Using the relationship $I_{signal} = I_{post-edge} - K * I_{pre-edge}$; where I_{signal} represents the intensity in the elemental map, $I_{post-edge}$ and $I_{pre-edge}$ the intensities in the filtered images registered before and on/after the ionization edge. The parameter K is a constant which translates the variation of the background at the $L_{2,3}$ ionization edge. For its estimation we have considered the ratio of the intensities in the two filtered images in an area where P is not present, with the carbon membrane that supports the nanoparticles. Another question that might arise is the variation of the constant K with the thickness. To answer to this question we have compared two different images: one which is calculated/defined by the ratio $\frac{I_{post-edge}}{I_{pre-edge}}$ pixel by pixel and translate the spatial variation of the constant K; and the second one is the thickness map defined by the ratio between the filtered and non-filtered images which represent the variation of the t/λ (t is the thickness and λ is the inelastic mean free path of electrons). By comparing the two parameters at the same area on

the carbon membrane for various tilt angles we traced the variation of K as a function of t/λ. **Figure S3.1** illustrates four points (1, 2, 3, 4) which were calculated for four different tilt angles. As can be observed when the carbon support was considered no variation of the constant thickness was detected. On the contrary, when the area was chosen on the particle, the ratio value for the minimum tilt angle (0°) was found to be equal to 0.28 (see point 5 shown in orange), above the value obtained in the case of carbon support, and for the maximum tilt angle a much higher value around 0.36 was found.

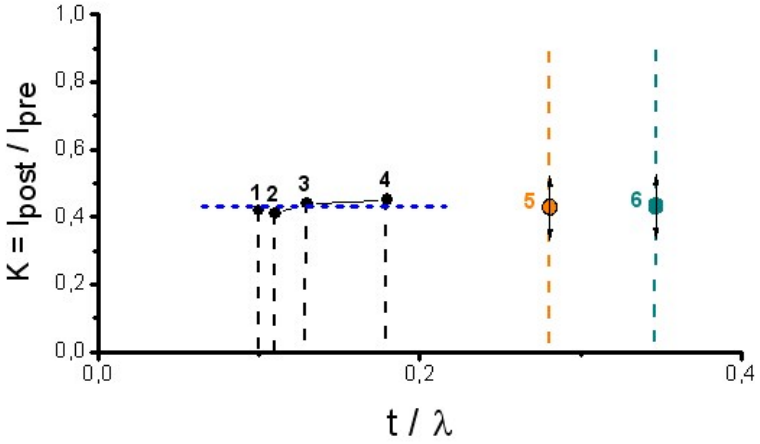

Figure S3.1: The variation of the K-factor as a function of the t/λ ratio; Both parameters were calculated for the same area defined on the carbon membrane in four different tilt angles (points 1, 2, 3, 4) and for the same area defined on the same particle for the minimum tilt angle (point 5) and for the maximum tilt angles (point 6). The K factor was defined as the ratio between the intensities of the images acquired before and after the P ionization edge. t represents the thickness and λ inelastic mean free path of electrons.

With these findings and knowing that for the spherical particles there is no variation of the thickness with the tilt angle there are two points that emerge: first, we probe the low thickness domains with a maximum ratio of 0.36 at 60 °; and second the K factor remains almost constant until t/λ= 0.2. The assumption that we can do at this stage is to consider in a first approximation, that the K factor is equal to 0.43, value calculated when the area was chosen on the membrane over the entire thickness of the respondents. The value of K=0.43 was used in the above relation of the phosphorus elemental projection tilt series.

SI 3.2: 2D versus 3D chemical mapping

To better illustrate and understand the gain in information obtained through a 2D elemental projection to 3D chemical volume, we can compare the chemical signals that both maps contain. Figure S3.2 shows a 2D elemental projection extracted from the two corresponding tilt series (ZL and P elemental projection tilt series) and a longitudinal slice taken at the same depth through the two corresponding reconstructed volumes (ZL and P chemical volume) for the same viewing direction. By comparing the intensity profiles plotted along a line through the two nanoparticles in both images one can observe that the signal to noise ratio (SNR) in the section extracted from the reconstructed chemical volume is higher than that corresponding to the 2D elemental projection. This facilitates the assignment of pixels belonging to the shell in areas where phosphorus is absent. If we look at the area between the two considered particles in which the shells of the particles are in contact (white rings), from the longitudinal slice the phosphorus absence within the shell is more evident by analyzing the intensity profile. Concerning the nanoparticle core, the P chemical signal plotted on the longitudinal slice is constant, reflecting thus its constant distribution, which is not the case on the 2D elemental projection that makes the interpretation more difficult.

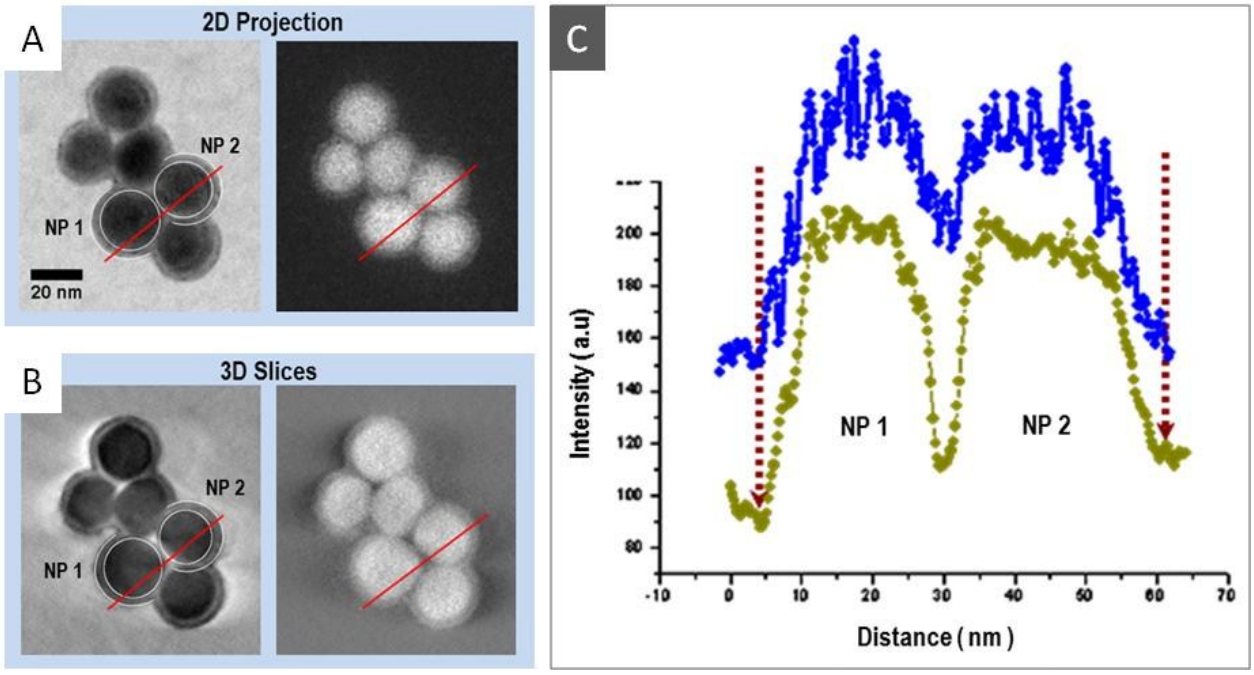

Figure S3.2: A) Images extracted for the same tilt angle from the ZL tilt series and 2D phosphorus elemental map. B) Longitudinal slices taken at the same depth from the two reconstructed volumes: Mean density (ZL reconstruction) and the Phosphorus chemical map that reflects its spatial distribution; C) intensity profiles plotted

along a line that crosses two nanoparticles (shown by the red line) on the 2D elemental map (blue) and on the slice extracted from the chemical volume (green). The red arrows indicate the nanoparticle's boundaries deducted from ZL images.

---

[1] W. Saxton, W. Baumeister, M. Hahn, *Ultramicroscopy,* 1984**,13,** 57–70.
[2] J.R. Kremer, D.N. Mastronarde, J.R. Mc Intosh, *J Struct Biol*, 1996, **116**, 71−76.
[3] R. Gordon, R. Bender, G.T. Herman, *J Theor Biol A*, 1970, **29**, 471−481.
[4] C. Messaoudi, T. Boudier, C.O.S. Sorzano, S. Marco, *BMC Bioinformatics*, 2007, **8**, 288.
[5] http://www.slicer.org/; Fedorov, A., Beichel, R., Kalpathy-Cramer, J., Finet, J., Fillion-Robin, J-C., Pujol, S., Bauer, C., Jennings, D., Fennessy, F., Sonka, M., Buatti, J., Aylward, S.R., Miller, J.V., Pieper, S., Kikinis, R. 3D Slicer as an Image Computing Platform for the Quantitative Imaging Network. *Magn Reson Imaging.* **30** (9), 1323-41 (2012)
[6] https://www.cgl.ucsf.edu; Pettersen, E.F., Goddard TD, Huang C.C., Couch, G.S., Greenblatt, D.M., Meng E.C., Ferrin, T.E. UCSF Chimera--a visualization system for exploratory research and analysis. *J Comput Chem.* **25** (13), 1605-12 (2004)
[7] Aronova M. A., Kim Y. C., Harmon R., Sousa A. A., Zhang G., Leapman R. D., Three-Dimensional elemental mapping of phosphorus by quantitative electron spectroscopic tomography QuEST, journal of Structural biology, **2007**, 160, 35-48.